

The impact of nonlinearity on degenerate parametric amplifiers

Jeffrey F. Rhoads^{1,a)} and Steven W. Shaw^{2,b)}

¹*School of Mechanical Engineering, Birck Nanotechnology Center, and Ray W. Herrick Laboratories, Purdue University, West Lafayette, Indiana 47907, USA*

²*Department of Mechanical Engineering, Michigan State University, East Lansing, Michigan 48824, USA*

(Received 2 March 2010; accepted 11 May 2010; published online 7 June 2010)

This work investigates the effects of system nonlinearities on degenerate parametric amplifiers. A simple, Duffing-type nonlinearity is appended to a representative equation of motion for a mechanical or electromechanical parametric amplifier, and classical perturbation methods are used to characterize the resulting effects on the amplifier's frequency response and performance. Ultimately, the work demonstrates that parametric amplification can be realized in nonlinear, dynamic-range limited systems, such as resonant micro- or nanosystems, but at the expense of performance degradation. Additionally, it is shown that nonlinear amplifiers can be operated above their linear instability threshold but that doing so results in bistable amplified responses. © 2010 American Institute of Physics. [doi:10.1063/1.3446851]

Degenerate parametric amplifiers based on resonant micro- and nanosystems have received significant attention in the applied physics and engineering research communities over the past few years due to their distinct utility in low-noise, low-distortion signal amplification.^{1–7} While these small-scale parametric amplifier implementations utilize modes of operation similar to those exploited by their more conventional electrical counterparts, in their most common micro/nanomechanical embodiments they also feature a scale-dependent dynamic range. Because of this, many small-scale parametric amplifiers exhibit a narrow window of forcing amplitude within which classical linear parametric amplification can be effectively realized.^{5–8} Accordingly, if low-noise, low-distortion signal amplification is to be fully exploited in future micro/nanoscale transducer designs, it may need to be realized in a nonlinear context.

The present work seeks to characterize the utility of degenerate parametric amplifiers operating within a nonlinear frequency response regime. Specifically, the work examines the behavior of a representative degenerate amplifier with a hardening, Duffing-type nonlinearity. A classical perturbation technique, the method of averaging, is used to recover pertinent performance metrics, including the amplifier's gain/pump and gain/phase characteristics, and these results are subsequently benchmarked against the metrics of a linear device.

Classical parametric amplifiers are linear resonators driven by a combined direct and parametric excitation. In conventional implementations, the direct excitation signal is targeted for amplification, and a time-varying system impedance serves as a parametric pump. While linearity can be maintained in systems with an appreciable dynamic range, many micro/nanoresonators, including those based on vibrating nanowires or nanotubes, operate in the presence of a relatively high noise floor and a reduced “nonlinear ceiling,”⁹ and when parametrically amplified exhibit a distinctly nonlinear, near-resonant response. While the origins of this nonlinearity vary from device to device and can stem from large

deflections or inertial, dissipative, and transduction effects, the singularly important nonlinear effect of frequency pulling can be generically characterized by appending a simple cubic term to a representative degenerate parametric amplifier model. With this in mind, the present effort considers a non-dimensional governing equation for a degenerate amplifier of the form

$$z'' + 2\varepsilon\zeta z' + z + \varepsilon\lambda \cos(2\Omega\tau)z + \varepsilon\alpha z^3 = \varepsilon\eta \cos(\Omega\tau + \phi), \quad (1)$$

where z represents the amplifier response, ζ captures the effects of linear dissipation attributable to, for example, fluid and/or material damping, λ represents the effective parametric pump amplitude, Ω dictates the system's excitation frequency, τ defines a nondimensional time variable, η specifies the direct excitation amplitude, and ϕ represents a relative phase term, introduced to account for the phase-dependent tuning of degenerate amplification. Note that for analytical purposes, all of the excitation, dissipation, and nonlinear terms included in Eq. (1) are assumed to be small, and are scaled by the small parameter ε for ease of analysis.

Equation (1) lacks a closed-form solution suitable for predictive design and analysis, but is amenable to perturbation methods, specifically, the method of averaging. In light of this, the system response is described in terms of slowly-varying coordinates by introducing a constrained coordinate transformation of the form

$$z(\tau) = X(\tau)\cos(\Omega\tau) + Y(\tau)\sin(\Omega\tau),$$

$$z'(\tau) = -X(\tau)\Omega \sin(\Omega\tau) + Y(\tau)\Omega \cos(\Omega\tau), \quad (2)$$

and a frequency detuning parameter σ , defined by

$$\sigma = \frac{\Omega - 1}{\varepsilon}, \quad (3)$$

into Eq. (1). The resulting equation and the implicit constraint [obtained by relating z and z' defined above, which requires that $X'(\tau)\cos(\Omega\tau) + Y'(\tau)\sin(\Omega\tau) = 0$], are solved for X' and Y' and averaged over one period $2\pi/\Omega$ of excitation. The resulting averaged equations are given by

^{a)}Electronic mail: jfrhoads@purdue.edu.

^{b)}Electronic mail: shawsw@egr.msu.edu.

$$\begin{aligned}
 X' &= -\frac{1}{8}\varepsilon(2\lambda Y + 8\sigma Y + 8\zeta X - 3\alpha X^2 Y - 3\alpha Y^3 \\
 &\quad - 4\eta \sin \phi) + \mathcal{O}(\varepsilon^2), \\
 Y' &= -\frac{1}{8}\varepsilon(2\lambda X - 8\sigma X + 8\zeta Y + 3\alpha X Y^2 + 3\alpha X^3 \\
 &\quad - 4\eta \cos \phi) + \mathcal{O}(\varepsilon^2).
 \end{aligned}
 \tag{4}$$

The system's steady-state behavior can be recovered from these equations by setting $(X', Y') = (0, 0)$ and solving for the steady-state values of X and Y , which are accurate to $\mathcal{O}(\varepsilon)$. The performance of the nonlinear amplifier can be examined by converting the result into polar (amplitude/phase) coordinates and evaluating pertinent metrics for various normalized pump amplitudes (λ), relative phase angles (ϕ), direct excitation amplitudes (η), and nonlinear stiffnesses (α). The amplifier gain is defined to be

$$G = \frac{a_1}{a_1|_{\lambda=0}}, \tag{5}$$

where a_1 represents the steady-state amplitude of the amplifier's maximum amplitude frequency response branch. A closed-form expression for G is omitted here due to its non-trivial dependence on system parameters.

The near-resonant response structure of this system is quite intricate, as now summarized using frequency response and phase plane diagrams derived using the averaged equations. Figure 1 depicts the response of a representative parametric amplifier driven at three distinct pump amplitudes. As evident from Fig. 1(a), when the amplifier of interest is driven below the system's parametric instability threshold (or Arnold tongue, specifically, for $\lambda < 4\zeta$ at $\sigma=0$), the system exhibits a classical Duffing-type response, which for positive values of the nonlinearity parameter α bends to the right. This resonance structure is attributable to the fact that there is a single "active" resonance at this operating condition—that associated with the system's direct excitation. Note that the inset shows the (X, Y) phase plane at the indicated frequency. Figures 1(b) and 1(c) depict the amplifier's near-resonant response when driven slightly above and well above the parametric instability threshold, respectively. It is evident that in each of these scenarios the response features five distinct response branches, three of which are stable. The two additional branches present here are comparable in magnitude but distinct in phase from the other stable/unstable upper branch response pair, and arise from a bifurcation across the instability threshold. This leads to the coexistence of two "active" stable resonances in the amplifier. One can view the transition from Fig. 1(a) to Fig. 1(c) as going from a Duffing-dominated response to a parametrically dominated response, albeit with broken symmetry arising from the direct excitation. Note that the amplifier's upper branch remains qualitatively unchanged regardless of whether the system is driven above or below the parametric instability threshold but that two slightly different stable responses may be observed. Because of this the parametric instability threshold for the pump amplitude is of only minor concern, in contrast with linear amplifier considerations.

Figure 2 highlights the gain versus normalized pump amplitude for a representative nonlinear amplifier driven at resonance. As evident, even comparatively small cubic nonlinearities limit the amplifier gain. Because of this, gains comparable in magnitude to those reported in prior literature

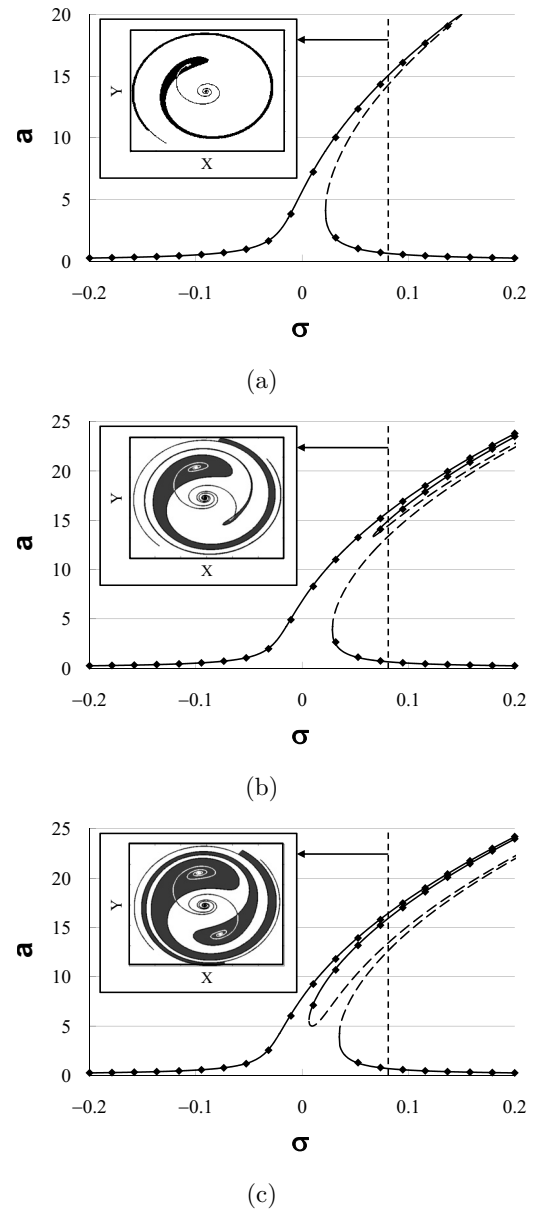


FIG. 1. Frequency response, a vs σ , for a representative amplifier ($\phi = -\pi/4$, $\eta = 0.1$, $\alpha = 0.001$, and $\zeta = 0.01$) driven (a) slightly below its parametric instability threshold ($\lambda = 0.03$), (b) slightly above its parametric instability threshold ($\lambda = 0.055$), and (c) well above its parametric instability threshold ($\lambda = 0.08$). Solid/dashed lines are used to indicate stable/unstable steady-state solutions. Data points are recovered from simulations of the original equation of motion, Eq. (1). Insets highlight the basins of attraction in the (X, Y) phase plane for $\sigma = 0.075$; alternating basins are shown in black and white, with internal trajectories (the unstable manifolds of the saddles) highlighted in the locally opposite colors.

are not expected to be obtainable in devices exhibiting even small levels of nonlinearity.¹⁻⁴ However, because the classical linear limitation on pump amplitude ($\lambda \approx 4\zeta$) can be largely disregarded in a nonlinear amplifier, meaningful gains can still be realized with strong pumping. Because of this, parametric amplification can be plausibly realized in a micro/nanoresonator with a limited, or even nonexistent, linear dynamic range.

Because the system of interest is designed to operate in a degenerate mode, a phase-dependent amplifier gain is predicted for all device implementations, including those operating within a linear, near-Lorentzian frequency response regime. Figures 3 and 4 highlight how the phase-periodic gain

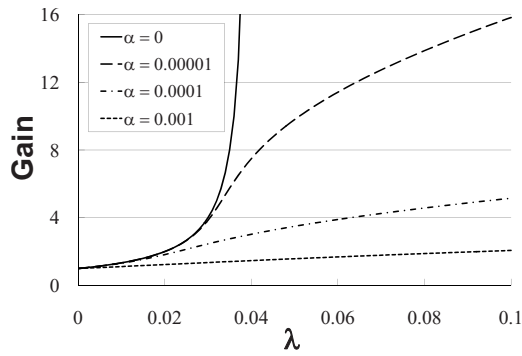


FIG. 2. Amplifier gain $G(\sigma=0)$ vs parametric pump amplitude λ for a representative amplifier with $\phi=-\pi/4$, $\eta=0.1$, and $\zeta=0.01$.

variance obtained in linear amplifiers is distorted in the presence of nonlinearity. Specifically, these results indicate that increasing the magnitude of the cubic stiffness nonlinearity results in additional asymmetry in the gain/phase relationship. Though this asymmetry ultimately has minimal effect on absolute system performance, it does alter the phase value at which maximum gains can be achieved, thus shifting the amplifier's optimal operating condition.

The aforementioned results clearly demonstrate that meaningful parametric amplification can be realized in resonant systems driven within a nonlinear response regime, albeit with performance metrics generally inferior to those seen in classical, linear parametric amplifiers. While this performance degradation is not desirable, parametric amplification does appear to be a feasible option for on-chip, low-noise, low-distortion amplification in dynamic-range limited

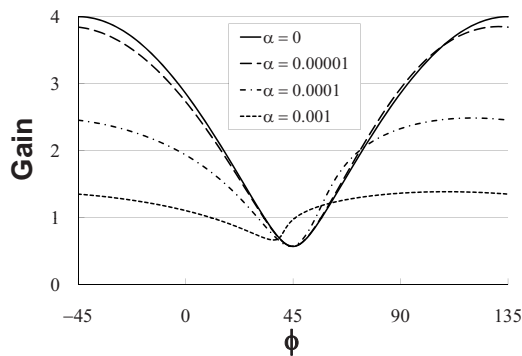


FIG. 3. Amplifier gain $G(\sigma=0)$ vs relative excitation phase ϕ for an amplifier with $\eta=0.1$, $\lambda=0.03$, and $\zeta=0.01$.

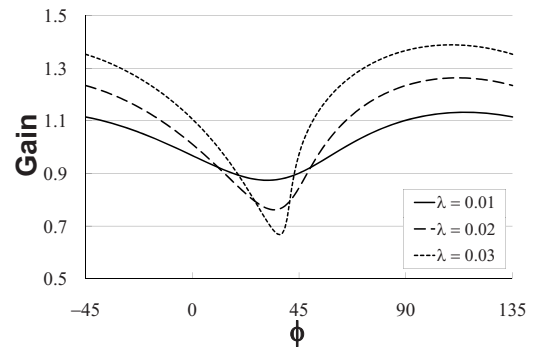


FIG. 4. Amplifier gain $G(\sigma=0)$ vs relative excitation phase ϕ for an amplifier with $\eta=0.1$, $\alpha=0.001$, and $\zeta=0.01$.

systems, such as resonant micro/nanotransducers, even into their nonlinear operating range. Ongoing research is aimed at realizing parametric amplification in two distinct classes of nanoresonators, both of which have been shown to exhibit a limited linear dynamic range: electrostatically actuated single-wall carbon nanotube and silicon nanowire resonators.

A preliminary version of this work appeared at the 2nd International Conference on Micro- and Nanosystems held as part of the 2008 American Society of Mechanical Engineers' International Design Engineering Technical Conference (IDETC2008).⁷ This work was supported by the Dynamical Systems Program of the National Science Foundation under Grant Nos. 0826276 and 0758419. The authors are grateful to Nick Miller for his assistance with the numerical simulations contained herein.

¹D. Rugar and P. Grütter, *Phys. Rev. Lett.* **67**, 699 (1991).

²D. W. Carr, S. Evoy, L. Sekaric, H. G. Craighead, and J. M. Parpia, *Appl. Phys. Lett.* **77**, 1545 (2000).

³A. Dăna, F. Ho, and Y. Yamamoto, *Appl. Phys. Lett.* **72**, 1152 (1998).

⁴M. Zalalutdinov, A. Olkhovets, A. Zehnder, B. Ilic, D. Czaplewski, H. G. Craighead, and J. M. Parpia, *Appl. Phys. Lett.* **78**, 3142 (2001).

⁵I. Mahboob and H. Yamaguchi, *Appl. Phys. Lett.* **92**, 173109 (2008).

⁶I. Mahboob and H. Yamaguchi, *Appl. Phys. Lett.* **92**, 253109 (2008).

⁷J. F. Rhoads and S. W. Shaw, *The Effects of Nonlinearity on Parametric Amplifiers*, IDETC/CIE 2008: The 2008 ASME International Design Engineering Technical Conferences, 2nd International Conference on Micro- and Nanosystems, 2008, Brooklyn, New York, DETC2008-49594.

⁸R. Lifshitz and M. C. Cross, *Review of Nonlinear Dynamics and Complexity*, edited by H. G. Schuster (Wiley, Weinheim, Germany, 2008), Vol. 1, p. 1.

⁹H. W. C. Postma, I. Kozinsky, A. Husain, and M. L. Roukes, *Appl. Phys. Lett.* **86**, 223105 (2005).